# Impact of capping agent removal from Au NPs@MOF core–shell nanoparticle heterogeneous catalysts

Shan Dai, Kieu Phung Ngoc, Laurence Grimaud, Sanjun Zhang, Antoine Tissot, Christian Serre

# Impact of the capping agent removal from Au NPs@MOF core-shell nanoparticles heterogeneous catalysts

Shan Dai,[a,c] Kieu Phung Ngoc,[a] Laurence Grimaud,[b] Sanjun Zhang,[c] Antoine Tissot,[a†] Christian Serre[a†]

[a.] *Institut des Matériaux Poreux de Paris, Ecole Normale Supérieure, ESPCI Paris, CNRS, PSL University, 75005 Paris, France.*
[b.] *Laboratoire de biomolécules (LBM), Département de chimie, Sorbonne Université, École Normale Supérieure, PSL University, Sorbonne Université, CNRS, 75005 Paris, France.*
[c.] *State Key Laboratory of Precision Spectroscopy, East China Normal University, No. 3663, North Zhongshan Road, Shanghai 200062, China.*
† antoine.tissot@ens.psl.eu; christian.serre@ens.psl.eu

## Abstract

Metal nanoparticles encased in a MOF shell have shown remarkable properties in catalysis due to potential synergistic effects. However, capping agents, commonly used to prepare these nanoparticles, lower their reactivity once embedded into the MOF. Here we present a new route to prepare Polyvinylpyrrolidone (PVP)-capped Au NPs@MOF-808 core-shell composites. Simultaneously, we show for the first time that the capping PVP can be easily removed by chemical treatment while maintaining the integrity of MOF shell. We finally show how this leads to a significant enhancement of the reactivity of Au NPs@MOF-808 composites for selective oxidation reactions.

## Introduction

Metal (e.g., Au, Pt, Pd) nanoparticles (MNPs), are often used to bring new functions to hybrid structures including chemical sensing,[1, 2] catalysis,[3, 4] and bioimaging[5, 6] thanks to their tailorable properties. The preparation of MNPs with a well-defined particle size distribution often requires their stabilization by the adhesion of organic species at their surface. In addition, this can prevent the targeting NPs from aggregation.[7] However, the molecules attached to the particle surface usually block the active sites of NPs, making the charge transfer between substrates and NPs difficult. Thus, removing the surface stabilizer is of importance, particularly for applications in catalysis.[8]

Zr(IV)-carboxylate Metal-organic frameworks (MOFs) are a subclass of solids in MOFs chemistry being regarded as very promising in catalysis due to their notable chemical and thermal stability.[9] For example, MOF-808 is a benchmark robust Zr(IV)-carboxylate MOF built with $Zr_6$ oxoclusters and trimesate ligand with a molar ratio in 1: 2, giving rise to a 6-connected-nodes-based 3D framework with 1.8 nm large pores.[10] The large aperture size of MOF-808, as well as the abundant open metal sites (when the coordinated species are removed), make it very promising for organic-phase heterogeneous catalysis applications.[11]

Incorporating MNPs into MOFs often endows novel functions for multiple applications, especially for catalysis due to potential host-guest synergetic effects.[12] Bottle-around-a-ship strategy refers to the method where a MOF shell is built on preformed core materials (e.g., MNPs) regardless of their shape, size and morphology. The resulting core-shell composites exhibit "empty" MOF pores, therefore making their overall surface area accessible, in sharp contrast to the conventional loading of MNPs in the pores of the pre-synthesized and activated MOFs.[13] A major challenge still remains in synthesizing core-shell composites due to the fast intrinsic nucleation of MOFs.[13] As such, to construct core-shell composites, the use of capping agents on the surface of NPs is often inevitable to counterbalance the mismatched lattice parameters and/or surface chemistry. To the best of our knowledge, the study of the removal of capping agents on MOF-based core-shell composites is still an unexplored topic. This is probably due to the limited chemical stability of the shell materials conventionally used (ZIF-8, HKUST-1) and/or the difficulty in quantifying organic stabilizers in a complex chemical environment.

Here, we report the first synthesis of a core-shell MNPs@MOF structure based on benchmark MOF-808 and ultra-small Au NPs via a room temperature assembly strategy (see Figure 1). The resulting Au NPs@MOF-808 displays a uniform Au NPs distribution. We subsequently show how the polyvinylpyrrolidone (PVP) can be removed from Au@MOF core-shell particles, here the Au NPs@MOF-808, using various physical or chemical treatments. The catalytic efficiency of the composite is then evaluated by using the oxidation of benzyl alcohol as model reaction. A promising impact on the removal of PVP is observed when using the double solvent method and hydrochloric acid (HCl) washing, leading to boosted reaction efficiency, in agreement with a better accessibility of the Au surface sites. This discovery paves the way for the preparation of capping agent free MNP@MOF composite with a high reactivity and selectivity.

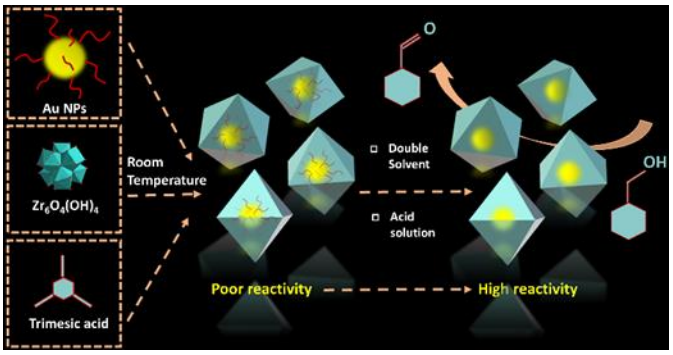


**Figure 1.** Schematic diagram for the assembly and PVP-removal of Au NPs@MOF-808 composite.

## Results and discussion

The catalyst fabrication (see Scheme 1) takes advantage of our previously reported two-steps room temperature synthesis of MOF-808 with small modifications.[14] PVP is a commonly used stabilizer in the preparation of MNPs for its role not only in the control of their size/shape but also in the prevention of their aggregation. Au was used as a model metal to investigate the removal of surface PVP due to its high reactivity for some standard catalytic reactions once the active sites are accessible. To construct the Au NPs@MOF-808 core-shell heterostructure, PVP is required on the surface of Au NPs to help them being well-dispersed in solution and efficiently adsorbed on the MOF crystal planes. As shown in Figure 2a, the prepared Au NPs displayed a polydispersed size, ranging from 1.2 to 3 nm (Figure S1). Note that the incorporation of such small-sized nanoparticles within Zr-MOFs is challenging due to the possible aggregation of Au NPs, particularly when using conventional solvothermal synthetic conditions that require elevated temperature. Furthermore, the Au NPs@MOFs core-shell architecture could help to prevent Au NPs aggregation when the PVP is removed due to the "compartment effect" from MOFs.

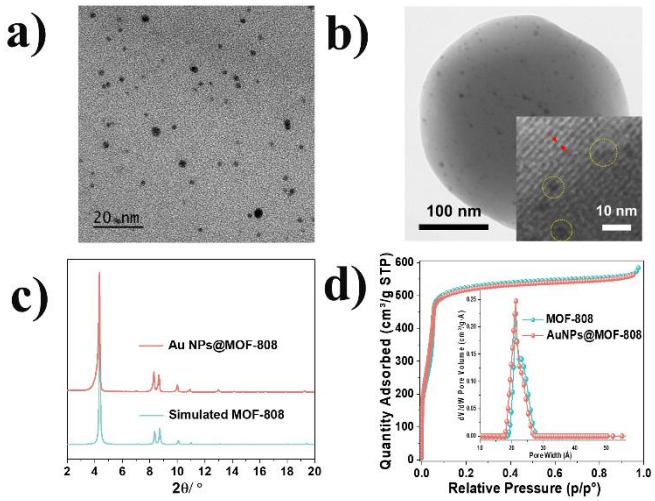


**Figure 2.** TEM images of a) the synthesized Au nanoparticles, b) the synthesized Au NPs@MOF-808 in large and small magnification; c) PXRD patterns ($\lambda_{Cu}$=1.5406Å) of Au NPs@MOF-808 in comparison with the simulated pattern of MOF-808; (d) 77K $N_2$ sorption isotherms of Au NPs@MOF-808 in comparison with the one of MOF-808 (pore size distribution as an inset).

For the synthesis of the composite, a solution of pre-formed $Zr_6$ oxoclusters in formic acid was added to well-dispersed Au NPs (in excess, 10 mM) in deionized water at room temperature, followed by the addition of 1,3,5-Benzenetricarboxylic acid (BTC). After overnight reaction under stirring, a well-defined core-shell structure was obtained after intensive washings (Figure 2b). The mean size of the encased Au NPs was 3 nm, which is slightly larger than the initial size. This could be due to the large pore size of MOF-808 (ca. 2 nm) that only allows the incorporation of Au NPs that are larger. Inductively coupled plasma-mass spectrometry (ICP-MS) on the obtained composites was used to evaluate the incorporated Au content (4.0/96.0, Au/Zr in atomic ratio), which is consistent with the value obtained by EDX analysis. The powder X-ray diffraction pattern (PXRD) in Figure 2c is in good agreement with the simulated pattern from the MOF-808 crystal structure, which confirms the crystallinity of Au NPs@MOF-808. As mentioned above, despite intensive $H_2O$ washings (20 times) to remove the excess Au NPs, the elemental mapping using ICP-MS (see Table S1), demonstrated that only 0.2% of Au was removed during this step, which further proved the formation of well-defined core-shell structure. $N_2$ porosimetry was conducted to investigate the porosity of the bare MOF-808 and the Au NPs@MOF-808 composites (Figure 2d), giving very close Brunauer-Emmett-Teller (BET) surface areas of 2100 $m^2/g$ for both materials, which could be due to the moderate Au

content in our case (4.0 atomic %). The pore size distribution analysis (Figure 2d) evidenced almost no change in agreement with the unique feature of the core-shell architecture, where the loaded guests does not occupy the pores of the MOF.[13]

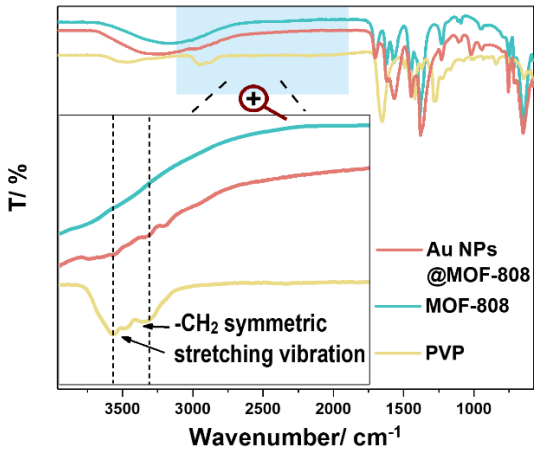


**Figure 3.** FT-IR spectra (T=298 K) of PVP, Au NPs@MOF-808, and bare MOF-808; inset: zoom in the blue area of the spectra.

Owing to the excess amount of PVP used in the synthesis of Au nanoparticles (Au/ PVP= 1: 100 molar ratio), the surface of Au NPs might be quantitatively covered at the end of the core-shell synthesis. Figure 3 shows the Fourier-transform infrared spectra (FT-IR) of the water-washed Au NPs@MOF-808, pure PVP, and bare MOF-808 respectively. In the case of Au NPs@MOF-808, the frequency of the $–CH_2$ symmetric stretching vibrational modes in the region of 3000-2800 $cm^{-1}$ that corresponds to the PVP reference confirms the existence of a significant amount of PVP left in the composites, which could exhibit a negative role in terms of catalytic activity due to the blocking of the accessible surface sites of nanoparticles.[15] However, analysing traces of PVP in a core-shell MOF-based composite using usual analytical methods such as NMR, FT-IR/Raman spectroscopies and TGA remains challenging. Thus, the presence of these residual species was assessed using a model catalytic reaction -the oxidation of benzyl alcohol (BA)- to evaluate the accessibility of the Au catalytic sites.[16] Since the size of BA is much smaller than the pore of MOF-808 (0.65 nm vs 1.8 nm), the diffusion of the BA is assumed not to limit the catalytic activity.

The model reaction is described Figure 4a. First, the BA oxidation efficiency of the pure MOF-808, pure Au NPs, and Au NPs@MOF-808 catalyst, before and after extensive water washing (20 times), was evaluated. As shown in Figure 4b (1-4), all these catalysts did not exhibit any reactivity (see the quantification in SI), indicating that i) the pure MOF-808 isn't active for this reaction and ii) the Au sites are inaccessible in both Au NPs and Au NPs@MOF-808 catalyst washed with water. Indeed, even though the PVP is highly hydrophilic, the washing with water of Au NPs and Au NPs@MOF-808 did not allow removing the capping agent, probably due to the very strong affinity of Au for PVP. These results thus demonstrate that the excess of PVP used for the Au nanoparticles synthesis indeed made the active Au sites inaccessible whatever inside the MOF shell or not.

Several studies have been reported regarding the removal of PVP from noble metal nanoparticles based composites but all of them were dealing with much more robust inorganic host matrices (e.g., silica, $TiO_2$, etc.).[8] Even though Zr-based MOFs like MOF-808 exhibit a relatively high chemical and thermal stability compared to other MOFs, it is still not comparable to these inorganic oxides. Therefore, more gentle ways need to be developed to remove PVP from NPs while protecting the MOF structure from degradation.

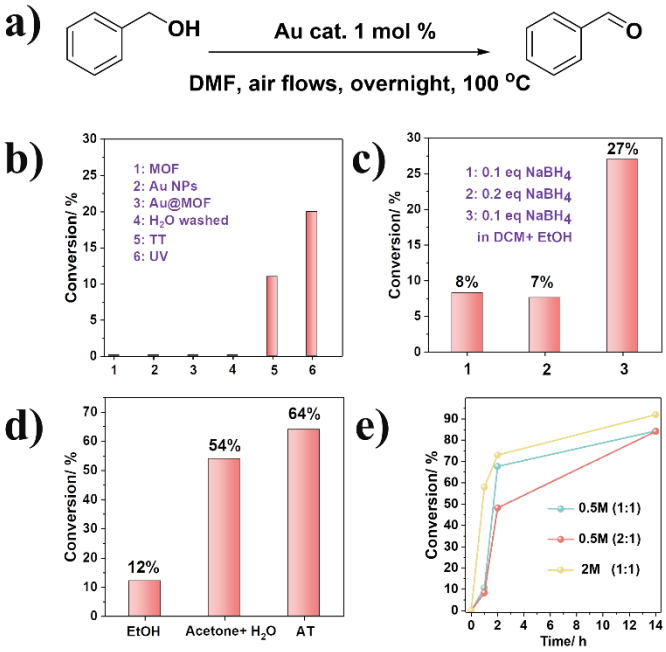


**Figure 4.** a) Model reaction and catalytic parameters used in this study b) BA oxidation achieved with different materials, pure MOF-808, pure Au NPs, Au NPs@MOF-808, water washed Au NPs@MOF-808, Au NPs@MOF-808 after thermal treatment (TT), and UV irradiation, c) Au NPs@MOF-808 treated with 0.1 eq. $NaBH_4$, 0.2 eq. $NaBH_4$ in acetone, and 0.1 eq. $NaBH_4$ in the mixture of DCM, d) BA oxidation achieved with Au NPs@MOF-808 treated with EtOH washing, the mixture of Acetone and $H_2O$ washing, and the acid washing, e) acid washing with different HCl concentrations and solvent ratios.

Thermal (TT)[17] and Ultraviolet (UV)[18] treatments where first applied to remove PVP. Thermal decomposition of PVP is usually performed between 200 and 350 ºC. The incorporation of the guest NPs in the MOF structure often decreases the thermal stability of the MOF. Our Au NPs@MOF-808 is thermally stable up to 225ºC under air (see Figure S6). We have thus treated the catalyst at 200°C for 5h but the conversion of BA was only 11% after 14h of reaction (Figure 4b (5)), which suggested that thermal treatment is not sufficient for the PVP removal. UV irradiation produces ozone upon interacting with molecular oxygen, which subsequently induces the oxidation of carbon-containing compounds into carbon dioxide and water and therefore the decomposition of PVP. However, the treatment under 257 nm irradiation led to a complete decomposition of the MOF structure even after 2h due to UV-induced linker degradation.[19] Alternatively, we used 365 nm UV irradiation to protect MOF from degradation. Unfortunately, PXRD (see Figure S7) evidenced a decrease of the crystallinity after 4h of exposure and only 20% of the BA conversion (Figure 4b (6)) was achieved.

$NaBH_4$ was then chosen for PVP removal inspired by Jongh et al. that have considered this treatment on dense $Au/TiO_2$ composites to displace PVP from Au NPs.[20, 21] Nevertheless, the treatment for $Au/TiO_2$ used either $H_2O$ or *tert*-butylamine (TBA), which is not suitable for MOF-808 due to the strong alkaline feature of TBA and $NaBH_4$ once dissolved in $H_2O$. Thus, treatments with different amounts of $NaBH_4$ were investigated preliminarily using an aprotic solvent (acetone). As shown in Figure 4c, the treatment with $NaBH_4$ indeed displayed improved catalytic efficiency as the treatment time increased. However, 0.2 eq $NaBH_4$ did not show any improved reactivity in comparison with 0.1 eq $NaBH_4$, indicating that a higher quantity of $NaBH_4$ did not lead to a satisfying reactivity. The treatment with 0.2 eq $NaBH_4$ for 2h did also lead to a loss of crystallinity as evidenced from a slight broadening of the Bragg peaks (see Figure S2) due to a partial degradation of MOF-808. The limited efficiency of varying treatments with $NaBH_4$ may also be due to the low solubility of $NaBH_4$ in acetone. Therefore, the treatment was subsequently carried out (with 0.1 eq of $NaBH_4$) in a more protic solvent (DCM/ethanol = 8.3:1 in volume). This is also required as acetone was shown to be reduced by $NaBH_4$ in the presence of alcohol.[22] After this new reduction assay at room temperature, the PXRD pattern of the composite showed its integrity was kept (see Figure S3). Interestingly, a pronounced catalytic enhancement using the treated catalyst reaching 27% conversion was observed after overnight reaction (Figure 4c (3)). We believe this could be due to a better removal efficiency of PVP associated with the better dissolution of $NaBH_4$ using a double solvent method (DSM). DSM represents the use of a mixture of good and poor solvent in an appropriate ratio to remove capping agents. The surface ligands tend to shrink on the surface of NPs to form compact configuration when the poor solvent is added, whilst they can be fully dispersed in the good solvent and therefore easy to detach from the particle surface. This dynamical process offers the opportunity to effectively remove the stabilizer. In order to verify our hypothesis, we treated the catalyst with 0.1eq $NaBH_4$ in ethanol. The PXRD of the catalyst after the treatment showed a significant decrease of crystallinity (Figure S4), while the catalytic activity did not exhibit any improvement, with only 12% of conversion after overnight reaction (Figure 4d (1)). Thus, it is likely that the mixed solvent is responsible for the reactivity improvement in the DCM/EtOH mixture. However, due to the high toxicity of DCM, alternative greener solvents shall be considered from a green/sustainable chemistry point of view. According to our hypothesis, one shall select a combination of a solvent that can fully dissolve PVP and another one not compatible with PVP. Accordingly, acetone and $H_2O$ were used instead of DCM and ethanol. The high-quality PXRD pattern (Figure S5) after overnight soaking indicated the intact structure of the treated catalyst. The subsequent catalytic test on the model reaction

gave a remarkable 54% conversion (Figure 4d (2)), much higher than the previous tests. This is in good agreement with the previous observation of the DSM effect on the PVP removal from Pt nanoparticles and nanocubes.[23, 24] In summary, the catalysts treated with $NaBH_4$ present a low reactivity and therefore, this approach was excluded from further study, while the DSM indeed displayed competitive advantage in both crystallinity preservation and efficiency enhancement.

Considering the fact that the PVP likely interacts with Au (0) species through Au-O or Au-N bond, one other plausible pathway to remove it from the gold surface is to use acidic compounds to protonate PVP, which thus makes the coordinating bonds weaker and PVP being more soluble in polar solvents.[25] In our case, since MOF-808 has a good stability in acidic media, we used 0.5M HCl acetone solution to treat the catalyst followed by a subsequent extensive acetone exchange to exclude the remaining species after treatment. Interestingly, BA oxidation experiment demonstrated reactivity enhancement (Figure 4d (3)), which reached 64% conversion. The structure stabilities after treatment and catalysis were evidenced by PXRD (see Figure S8).
DSM and acidic treatments routes therefore both showed a very positive impact on the composite reactivity. Notably, both of these methods have excellent compatibility with MOF-808. In the next step, we combined the DSM and acidic treatment using 0.5 M HCl in a mixture of acetone and $H_2O$ (in 1: 1 vol%) at room temperature. We then analysed the reaction kinetics and showed that the treated catalyst could induce up to 80% conversion (Figure 4e). Even though a higher acetone: $H_2O$ volume ratio was used in reference 24, a 2: 1 ratio did not result in an enhanced efficiency and final conversion after 24h in our case. As the Zr-MOFs are known to be highly stable in acidic media, a 2M HCl solution was also selected. The catalytic test in Figure 4e exhibited an even higher reactivity as well as faster kinetics, reaching 73% and 92% conversion in 2h and 14h, respectively. The PXRD measurement (Figure S9) and ICP-MS analysis (Table S1) both revealed the overall integrity of composites were maintained. This indicates that combining an acidic treatment with DSM is an ideal method for the removal of PVP from core-shell Au NPs@MOF-808 composites. Interestingly, no $-CH_2$ symmetric stretching vibrational peaks were observed in the treated composites (Figure S10), indicating the excellent removal of PVP, in good accordance with the catalytic results.

## Conclusions

As conclusion, for the first time, a core-shell architecture based on MOF-808 was synthesized with ultra-small Au NPs. The room temperature aqueous solution based synthesis allowed the encapsulation in green manner without Au NPs aggregation. Subsequently, the successful removal of the PVP from the Au NPs@MOF-808 composite was achieved following a double solvent method (DSM) under acidic conditions, leading to a highly active catalyst for benzyl alcohol oxidation. This work will guide future works towards the design of new generations of efficient metal nanoparticles@MOF composites for heterogeneous catalysis.

## Author Contributions

S.D., A.T., and C.S. conceived the idea; S.D. and K.N. performed all the experiments; L.G. helped to design the catalytic experiments; S.D. analysed the data and prepared the original manuscript; A.T. and C.S. managed the project; all authors contributed to discussion and paper revisions.

## Conflicts of interest

There are no conflicts to declare.

## Acknowledgements

S. D. is grateful for the support from CSC grant (grant number 201706140196). S.D. appreciates Dr. Xiangzhen Xu and Dr. Mathilde Lepoitevin for TEM measurements. Authors thank Bernard Goetz for the ICP-MS measurements.

## Notes and references

1. J. H. Fu, Z. Zhong, D. Xie, Y. J. Guo, D. X. Kong, Z. X. Zhao, Z. X. Zhao and M. Li, *Angew. Chem. Int. Edit.*, 2020, **59**, 20489-20498.
2. M. Weber, J. Y. Kim, J. H. Lee, J. H. Kim, I. Iatsunskyi, E. Coy, P. Miele, M. Bechelany and S. S. Kim, *J. Mater. Chem. A*, 2019, **7**, 8107-8116.
3. D. Munoz-Santiburcio, M. F. Camellone and D. Marx, *Angew. Chem. Int. Edit.*, 2018, **57**, 3327-3331.
4. L. C. Liu and A. Corma, *Chem. Rev.*, 2018, **118**, 4981-5079.
5. Y. Chen, H. R. Chen, D. P. Zeng, Y. B. Tian, F. Chen, J. W. Feng and J. L. Shi, *ACS Nano*, 2010, **4**, 6001-6013.
6. X. H. Huang, P. K. Jain, I. H. El-Sayed and M. A. El-Sayed, *Lasers Med. Sci.*, 2008, **23**, 217-228.

7. X. Wang, J. Zhuang, Q. Peng and Y. D. Li, *Nature*, 2005, **437**, 121-124.
8. Z. Q. Niu and Y. D. Li, *Chem. Mater.*, 2014, **26**, 72-83.
9. Y. Bai, Y. B. Dou, L. H. Xie, W. Rutledge, J. R. Li and H. C. Zhou, *Chem. Soc. Rev.*, 2016, **45**, 2327-2367.
10. H. Furukawa, F. Gandara, Y. B. Zhang, J. C. Jiang, W. L. Queen, M. R. Hudson and O. M. Yaghi, *J. Am. Chem. Soc.*, 2014, **136**, 4369-4381.
11. S. Y. Moon, Y. Y. Liu, J. T. Hupp and O. K. Farha, *Angew. Chem. Int. Edit.*, 2015, **54**, 6795-6799.
12. Q. H. Yang, Q. Xu and H. L. Jiang, *Chem. Soc. Rev.*, 2017, **46**, 4774-4808.
13. S. Dai, A. Tissot and C. Serre, *Adv. Energy Mater.*, DOI: 10.1002/aenm.202100061.
14. S. Dai, C. Simms, I. Dovgaliuk, G. Patriarche, A. Tissot, T. N. Parac-Vogt and C. Serre, *Chem. Mater.*, 2021, **33**, 7057-7066.
15. T. H. Yang, Y. Shi, A. Janssen and Y. Xia, *Angew. Chem. Int. Edit.*, 2020, **59**, 15378-15401.
16. C. Della Pina, E. Falletta and M. Rossi, *Chem. Soc. Rev.*, 2012, **41**, 350-369.
17. C. Prossl, M. Kubler, M. A. Nowroozi, S. Paul, O. Clemens and U. I. Kramm, *Phys. Chem. Chem. Phys.*, 2021, **23**, 563-573.
18. R.-Y. Zhong, K.-Q. Sun, Y.-C. Hong and B.-Q. Xu, *ACS Catal.*, 2014, **4**, 3982-3993.
19. D. Mateo, A. Santiago□Portillo, J. Albero, S. Navalón, M. Alvaro and H. García, *Angew. Chem.*, 2019, **131**, 18007-18012.
20. B. Donoeva and P. E. de Jongh, *ChemCatChem*, 2018, **10**, 989-997.
21. M. Luo, Y. Hong, W. Yao, C. Huang, Q. Xu and Q. Wu, *J. Mater. Chem. A*, 2015, **3**, 2770-2775.
22. H. C. Brown, E. J. Mead and B. C. S. Rao, *J. Am. Chem. Soc.*, 1955, **77**, 6209-6213.
23. R. M. Arán-Ais, F. J. Vidal-Iglesias, J. Solla-Gullón, E. Herrero and J. M. Feliu, *Electroanalysis*, 2015, **27**, 945-956.
24. I. A. Safo, C. Dosche and M. Oezaslan, *Z. Phys. Chem.*, 2018, **232**, 1319-1333.
25. G. Lee, J. H. Shim, H. Kang, K. M. Nam, H. Song and J. T. Park, *Chem. Commun.*, 2009, **33**, 5036-5038.